Spectral Efficiency Analysis of Uplink-Downlink Decoupled Access in C-V2X Networks

Luofang Jiao*, Kai Yu*, Yunting Xu*, Tianqi Zhang*, Haibo Zhou*, and Xuemin (Sherman) Shen†
*School of Electronic Science and Engineering, Nanjing University, Nanjing, China, 210023
Email: luofang_jiao@foxmail.com, kaiyu@smail.nju.edu.cn, yuntingxu@smail.nju.edu.cn,
tianqizhang@smail.nju.edu.cn, haibozhou@nju.edu.cn
†Department of Electrical and Computer Engineering, University of Waterloo, 200 University Avenue West,
Waterloo, Ontario, Canada, N2L 3G1. Email: sshen@uwaterloo.ca

***Abstract*—The uplink (UL)/downlink (DL) decoupled access has been emerging as a novel access architecture to improve the performance gains in cellular networks. In this paper, we investigate the UL/DL decoupled access performance in cellular vehicle-to-everything (C-V2X). We propose a unified analytical framework for the UL/DL decoupled access in C-V2X from the perspective of spectral efficiency (SE). By modeling the UL/DL decoupled access C-V2X as a Cox process and leveraging the stochastic geometry, we obtain the joint association probability, the UL/DL distance distributions to serving base stations and the SE for the UL/DL decoupled access in C-V2X networks with different association cases. We conduct extensive Monte Carlo simulations to verify the accuracy of the proposed unified analytical framework, and the results show a better system average SE of UL/DL decoupled access in C-V2X.**

***Index Terms*—C-V2X, uplink/downlink decoupled access, association probability, spectral efficiency, stochastic geometry.**

I. Introduction

WITH the rapid development of the cellular vehicle-to-everything (C-V2X) networks, it is of critical significance to enable high quality of service (QoS) of uplink (UL) and downlink (DL) for supporting the emerging advanced vehicular applications, such as stream media, autonomous vehicles and intelligent transportation systems (ITS) [1], [2]. Nevertheless, to satisfy the ever-increasing coverage demand and the more stringent service requirements of vehicle users, C-V2X is gradually evolving into a more complicated heterogeneous network composition, which is consisted of the macro base stations (MBS) and the small base stations (SBS) [3], [4]. However, the traditional user association and access mode suffer frequent network handover and low throughput for C-V2X networks [4]. It is widely accepted that the users located on the edge of SBS choose to access SBS in UL and access to MBS in DL can significantly increase UL rates in heterogeneous networks in cellular networks [5], [6], [7]. It is critical for the high UL rates guarantee such as sharing of security information and remote driving in C-V2X [8], [9]. Therefore, it is meaningful to study the impact of novel access technologies with flexible user association in heterogeneous C-V2X networks.

Different from the traditional coupled access technologies, the UL/DL decoupled access technology, where the UL and DL is separately access to any two different tiers of base stations (BS) (i.e., MBS and SBS), has been proved that it can bring significant gains in terms of coverage, throughput and load balancing, etc. [3], [10]. For example, Zhang *et al*. theoretically validated the UL performance improvement brought about by the UL/DL decoupled access over the conventional coupled UL/DL access mode [11]. Li *et al*. revealed the superiority of decoupled mode in multiuser multiple-input multiple-output (MIMO) heterogeneous networks in [5]. And Smiljkovikj *et al*. provided the mathematical expressions for various parameters of a decoupled two-tier network with macro cells and small cells in [12]. Sattar *et al*. in [10] made an in-depth analysis of spectral efficiency (SE) of all links from the perspective of joint association cases leveraging stochastic geometry. Furthermore, regarding UL/DL decoupled access in C-V2X networks, Yu *et al*. introduced the UL/DL decoupled access into C-V2X for the first time and proved that this technology could improve the UL's throughput and load balancing in C-V2X [7].

Although the UL/DL decoupled access has emerged as a novel and flexible access scheme to improve the C-V2X network performance, how to conduct a unified and joint UL/DL analysis is critical for evaluating the quality of emerging advanced C-V2X applications. Generally, the joint association probability, the UL/DL distance distributions to serving BSs and the SE of the UL/DL decoupled access in C-V2X networks are of important research significance and attract lots of academic attention. And in C-V2X, Chetlur *et al*. modeled the C-V2X as a Cox process [13] and characterized the coverage probability and derived the rate in [14]. Qian *et al*. considered the C-V2X in a multi-mode spectrum sharing scenario and derived the coverage probability and rate of vehicle users in [15]. Sial *et al*. presented a model of V2X over shared channels based on stochastic geometry [16].

In this paper, we propose a unified analytical framework and investigate the characteristics of the UL/DL decoupled access by leveraging the tool of stochastic geometry in C-V2X networks. We first model the C-V2X networks as a Cox process. Subsequently,, we leverage the stochastic geometry to derive the joint association probability and distance distributions to serving BSs. Moreover, the expressions of SE for the UL/DL decoupled access in C-V2X networks with different association cases are derived. We highlight our contributions in this paper as follows:

- We introduce the UL/DL decoupled access technology into C-V2X networks to better support C-V2X applications. Through modeling the UL/DL decoupled access C-V2X as a Cox process, a unified analytical framework is presented.
- We provide an in-depth theoretical analysis by the stochastic geometry, including the joint association probability, the UL/DL distance distributions to serving BSs, and the mathematical expressions of SE for different association cases in C-V2X networks.
- We conduct extensive Monte Carlo experimentation to verify the effectiveness of the proposed unified analytical framework and the simulation results provide a general guidance for the UL/DL decoupled access scheme in C-V2X networks.

The rest of this paper is organized as follows. Section II introduces the network model. In Section III, we give the problem formulation, analysis, solutions and proofs. The numerical and simulation results are presented and discussed in Section IV. Finally, we conclude this paper in Section V.

II. SYSTEM MODEL

A. Network Model

We model a two-tier UL/DL decoupled C-V2X network, which consists of SBS and MBS deployed in terms of an independent homogeneous Poisson point process (PPP) Φ of density λ in the Euclidean plane.

As shown in Fig.1, the UL/DL decoupled association process has four cases:

- Case 1: UL = MBS, DL = MBS
- Case 2: UL = SBS, DL = MBS
- Case 3: UL = MBS, DL = SBS
- Case 4: UL = SBS, DL = SBS

According to the characteristics of C-V2X [13], the MBSs are evenly distributed in the C-V2X networks while the SBSs are distributed along the roads. All BSs are deployed in a circular area with a radius of r. A road that passes through the origin is called the typical line and the roads that don't pass through the origion are called the other lines. We choose a vehicle on the typical lines as the typical vehicle. Φ_n denotes the set of BSs in terms of PPP with density λ_n, where $n \in \{M, S\}$ for MBS and SBS, respectively. We use $\Xi_{l_0}^{(S)}$ to denote the set of vehicles in the typical line l_0.

The MBS chooses to transmit to vehicles in typical line and other lines in the same power. The SBS uses beamforming and the directional antenna points to the typical line with a higher gain and transmits power to vehicles in other lines with a small gain. Therefore, the DL transmit power is the signal receiving power of the vehicles, and the UL transmit power is the signal receiving power of the MBSs and SBSs. The DL transmit power can be written as

$$P_{r,V} = \begin{cases} P_M G_M H_M \chi_M \|x\|^{-\alpha_M}, & x \in \Phi_M \\ P_S G_{S,0} H_{S,0} \chi_{S,0} \|x\|^{-\alpha_S}, & x \in \Xi_{l_0}^{(S)} \\ P_S G_{S,1} H_{S,1} \chi_{S,1} \|x\|^{-\alpha_S}, & x \in \Phi_S \backslash \Xi_{l_0}^{(S)}, \end{cases}$$

the UL transmit power can be written as

$$P_{r,M} = P_V G_{V,1} H_{V,1} \chi_M \|x\|^{-\alpha_M}, \quad x \in \Phi_M ,$$

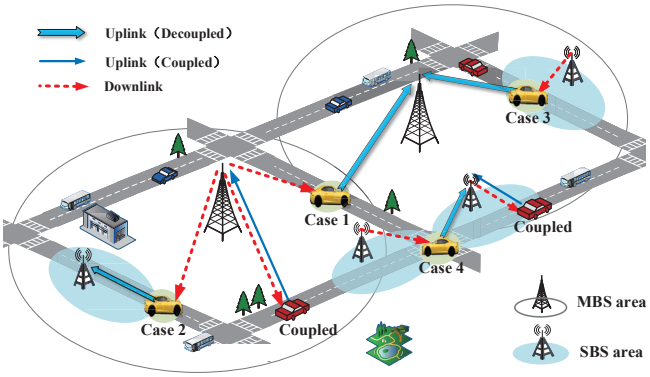

Fig. 1. Illustration of UL/DL decoupled access in C-V2X networks.

$$P_{r,S} = \begin{cases} P_V G_{V,0} H_{V,0} \chi_{S,0} \|x\|^{-\alpha_S}, & x \in \Xi_{l_0}^{(S)} \\ P_V G_{V,1} H_{V,1} \chi_{S,1} \|x\|^{-\alpha_S}, & x \in \Phi_S \backslash \Xi_{l_0}^{(S)}, \end{cases}$$

where x is the distance between vehicle and BS. The $P_{r,V}$, $P_{r,M}$ and $P_{r,S}$ are the signal receiving power of vehicle, MBS and SBS. P_V, P_M and P_S are the transmit power of vehicle, MBS and SBS. G_M, $G_{S,1}$ and $G_{S,0}$ are the antenna gains of MBS, SBS that transmits power to vehicle in other lines, SBS that transmits power to vehicle in typical line. $G_{V,0}$ and $G_{V,1}$ are the antenna gains of vehicle that transmits power to SBS and MBS. χ_M, $\chi_{S,0}$ and $\chi_{S,1}$ are the shadowing effects follow a log-normal distribution [14]. The power-law path loss parameters are exponent α_M and α_S ($\alpha > 2$). H_M, $H_{S,0}$, $H_{S,1}$, $H_{V,0}$ and $H_{V,1}$ are the channel fading gains of Nakagamim with parameter m_M, m_S, $m_{S,1}$, m_V and $m_{V,1}$. The fading gains H_i, where $i \in \{M, (S,0), (S,1), (V,0), (V,1)\}$, follow a Gamma distribution and its probability density function (PDF) is

$$f_{H_i} = \frac{m_i^{m_i} h^{m_i - 1}}{\Gamma(m_i)} exp(-m_i h) \quad m \in \{m_M, m_{S,0}, m_{S,1}\}.$$

B. Association Policy for BSs and vehicles

We assume that a vehicle is associated with the MBS/SBS which yields the highest biased received power in DL, similarly, the MBS/SBS will serve the vehicle with the highest biased transmit power in UL, namely the vehicles in the Voronoi cell of a BS connect to it. To handle the effect of shadowing, we use displacement theorem to express it as a random displacement of the location of the typical receiver [14]. Thus, $P_r(x) = PG\chi\|x\|^{-\alpha}$ can be written as $P_r(y) = PG\|y\|^{-\alpha}$, where $y = \chi^{-\frac{1}{\alpha}} x$, then the transformed points form a 2D homogeneous PPP with intensity λ to $E\left[\chi^{-\frac{2}{\alpha}}\right]\lambda$, the 1D PPP's intensity is λ to $E\left[\chi^{-\frac{1}{\alpha}}\right]\lambda$. Therefore, we use λ_L, λ_M, λ_S, λ_V to denote the transformed λ_l, λ_m, λ_s, λ_v, respectivily. In $\Phi_S \backslash \Xi_{l_0}^{(S)}$, using the Theorem 1 in [14], the vehicles and SBSs form 2D PPP with intensity $\lambda_{Sa} = E\left[\chi_{S,1}^{-\frac{2}{\alpha}}\right]\pi\lambda_l\lambda_s$, $\lambda_{Va} = E\left[\chi_{S,1}^{-\frac{2}{\alpha}}\right]\pi\lambda_l\lambda_v$, respectively.

The typical vehicle associates with a MBS in DL if

$$P_M G_M B_M \|x_M\|^{-\alpha_M} > P_S G_{S,0} B_S \|x_S\|^{-\alpha_S}, \qquad (1)$$

where B is selection bias factor. Otherwise, the vehicle connects to a SBS.

Similarly, the typical vehicle associates with a MBS in UL if

$$P_V G_{V,1} \|x_M\|^{-\alpha_M} > P_V G_{V,0} \|x_S\|^{-\alpha_S}. \tag{2}$$

Otherwise, the typical vehicle associates with a SBS. We denote $A_{M,S} = P_M G_M B_M / P_S G_{S,0} B_S$, $B_{M,S} = P_V G_{V,1} / P_V G_{V,0}$, substituting for (1) and (2):

$$A_{M,S} \|x_M\|^{-\alpha_M} > \|x_S\|^{-\alpha_S}, \tag{3}$$

$$B_{M,S} \|x_M\|^{-\alpha_M} > \|x_S\|^{-\alpha_S}, \tag{4}$$

the transmit power of MBS is much larger than SBS and vehicle, $A_{M,S}$ is larger than $B_{M,S}$.

C. Interference for UL and DL

In DL, the aggregate interference at the typical vehicle includes the interference from the MBSs I_M, the interference from the SBSs in the typical line $I_{S,0}$ and the interference from the SBSs in other lines $I_{S,1}$. In UL, the aggregate interference includes the interference from the vehicles in the typical line $I_{V,0}$ and the interference from the vehicles in the other lines $I_{V,1}$. Therefore, the SINR in DL is

$$SINR_D = \frac{P(X^*)}{I_M + I_{S,0} + I_{S,1} + \sigma_D^2}. \tag{5}$$

The SINR measured in UL is

$$SINR_U = \frac{P(X^*)}{I_{V,0} + I_{V,1} + \sigma_U^2}, \tag{6}$$

where X^* denotes the max power location. Because the system is interference-limited and the noise is much smaller than the interference [13], the thermal noise is neglected, $\sigma_U^2 = \sigma_D^2 = 0$.

III. SPECTRAL EFFICIENCY ANALYSIS

In this section, we derive the joint association probabilities for UL/DL decoupled C-V2X using stochastic geometry. Based on the above analysis, the SE of each link in UL/DL decoupled access C-V2X can be derived.

A. Association Probability

According to the null probability of 1D and 2D PPP [13], the cumulative distribution functions (CDF) of x_S, x_M are

$$F_S(x_S) = 1 - \exp(-2\lambda_S x_S), \tag{7}$$

$$F_M(x_M) = 1 - \exp\left(-\lambda_M \pi x_M^2\right). \tag{8}$$

According to $f(x) = \mathrm{d}F(x)/\mathrm{d}x$, the probability density functions (PDF) of x_S, x_M are

$$f_S(x_S) = 2\lambda_S \exp(-2\lambda_S x_S), \tag{9}$$

$$f_M(x_M) = 2\pi x_M \lambda_M \exp\left(-\lambda_M \pi x_M^2\right). \tag{10}$$

According to the association policy given by (3) and (4), we derive the joint association probability as follows:

1) Case 1: The probability that the typical vehicle connects to MBSs both in DL and UL is

$$\Pr(Case\,1) = \Pr\left(A_{M,S} X_M^{-\alpha_M} > X_S^{-\alpha_S}; B_{M,S} X_M^{-\alpha_M} > {X_S}^{-\alpha_S}\right). \tag{11}$$

According to the consideration of $A_{M,S} > B_{M,S}$, the above formula can be written as

$$\Pr(Case\,1) = \Pr\left(X_M < B_{M,S}^{\frac{1}{\alpha_M}} X_S^{\frac{\alpha_S}{\alpha_M}}\right). \tag{12}$$

The joint association probability of Case 1 is

$$\Pr(Case\,1) = 1 - \int_0^\infty \left[2\lambda_S \exp\left(-\lambda_M \pi B_{M,S}^{\frac{2}{\alpha_M}} x_S^{\frac{2\alpha_S}{\alpha_M}} - 2\lambda_S x_S\right)\right] dx_S, \tag{13}$$

when $\alpha_S = \alpha_M$, $\Pr(Case\,1)$ in closed form is

$$\Pr(Case\,1) = 1 - \sqrt{\frac{\lambda_S^2}{\lambda_M B_{M,S}^{\frac{2}{\alpha}}}} \exp\left(\frac{\lambda_S^2}{\lambda_M \pi B_{M,S}^{\frac{2}{\alpha}}}\right) erfc\left(\frac{\lambda_S}{\sqrt{\lambda_M \pi B_{M,S}^{\frac{2}{\alpha}}}}\right). \tag{14}$$

2) Case 2: The probability that the typical vehicle connects to SBS in UL and MBS in DL is

$$\begin{aligned}\Pr(Case\,2) &= \Pr\left(A_{M,S} X_M^{-\alpha_M} > X_S^{-\alpha_S}; B_{M,S} X_M^{-\alpha_M} < X_S^{-\alpha_S}\right) \\ &= \Pr\left(B_{M,S} X_M^{-\alpha_M} < X_S^{-\alpha_S} < A_{M,S} X_M^{-\alpha_M}\right).\end{aligned} \tag{15}$$

The joint association probability of Case 2 is formulated as

$$\begin{aligned}\Pr(Case\,2) &= \int_0^\infty \left[2\lambda_S \exp\left(-\lambda_M \pi B_{M,S}^{\frac{2}{\alpha_M}} x_S^{\frac{2\alpha_S}{\alpha_M}} - 2\lambda_S x_S\right)\right] dx_S \\ &\quad - \int_0^\infty \left[2\lambda_S \exp\left(-\lambda_M \pi A_{M,S}^{\frac{2}{\alpha_M}} x_S^{\frac{2\alpha_S}{\alpha_M}} - 2\lambda_S x_S\right)\right] dx_S.\end{aligned} \tag{16}$$

3) Case 3: The probability that the typical vehicle connects to MBS in UL and SBS in DL is

$$\Pr(Case\,3) = \Pr\left(A_{M,S} X_M^{-\alpha_M} < X_S^{-\alpha_S}; B_{M,S} X_M^{-\alpha_M} > {X_S}^{-\alpha_S}\right), \tag{17}$$

because $A_{M,S} > B_{M,S}$, the domain in (17) is empty, $\Pr(Case\,3) = 0$, which means that Case 3 won't happen. Therefore, we will not discuss Case 3 in later sections.

4) Case 4: The probability that the typical vehicle connects to SBS both in UL and DL is:

$$\begin{aligned}\Pr(Case\,4) &= \Pr\left(A_{M,S} X_M^{-\alpha_M} < X_S^{-\alpha_S}; B_{M,S} X_M^{-\alpha_M} < {X_S}^{-\alpha_S}\right) \\ &= \Pr\left(X_S < A_{S,M}^{\frac{1}{\alpha_S}} X_M^{\frac{\alpha_M}{\alpha_S}}\right),\end{aligned} \tag{18}$$

The joint association probability of Case 4 is formulated as

$$\begin{aligned}&\Pr\left(Case\,4\right)\\&=\int_0^\infty\left[2\lambda_S\exp\left(-\lambda_M\pi A_{M,S}^{\frac{2}{\alpha_M}}x_S^{\frac{2\alpha_S}{\alpha_M}}-2\lambda_S x_S\right)\right]dx_S.\end{aligned}\tag{19}$$

Proof: Due to space constraints, we take the proof of Case 1 as an example. The proof of joint association probability of Case 1 (UL=DL=MBS) is

$$\begin{aligned}&\Pr\left(Case\,1\right)\\&=Pr(B_{M,S}X_M^{-\alpha_M}>X_S^{-\alpha_S})\\&=E_{X_S}\left[\Pr\left(X_M<B_{M,S}^{\frac{1}{\alpha_M}}x_S^{\frac{\alpha_S}{\alpha_M}}\,|X_S\right)\right]\\&=\int_0^\infty F_M\left(B_{M,S}^{\frac{1}{\alpha_M}}x_S^{\frac{\alpha_S}{\alpha_M}}\right)f_S\left(x_S\right)dx_S\\&\overset{(a)}{=}1-\int_0^\infty\left[2\lambda_S\exp\left(-\lambda_M\pi B_{M,S}^{\frac{2}{\alpha_M}}x_S^{\frac{2\alpha_S}{\alpha_M}}-2\lambda_S x_S\right)\right]dx_S,\end{aligned}\tag{20}$$

where (a) follows from the substituting $F_M\left(\cdot\right)$ and $f_S\left(\cdot\right)$ from Eq. (8) and Eq. (9) in the previous steps. And the special case $\alpha_S=\alpha_M$ can follow the proof of Lemma 2 in [14].

Similarly, the proofs of other joint association probabilities can be derived by following the steps as Case 1. ■

B. Distance Distribution of A Vehicle to Serving BSs

The exact expressions of distance distributions to serving BSs of a vehicle for three cases are derived in this section. Because Case 1's and Case 4's UL and DL are associated with the same type BSs, Case 1's and Case 4's distance distributions are only one type. While Case 2's UL and DL connect to different types of BSs, there are two types of distance distributions to consider.

1) The distance distribution of Case 1 is formulated as

$$f_{X_M|Case\,1}=\frac{\exp\left(-\lambda_S\pi 2B_{S,M}^{\frac{1}{\alpha_S}}x^{\frac{\alpha_M}{\alpha_S}}\right)f_{X_M}\left(x\right)}{\Pr\left(Case\,1\right)}.\tag{21}$$

2) The distance distribution of Case 2 is formulated as

$$\begin{aligned}f_{X_M|Case\;2}=&\frac{f_{X_M}\left(x\right)}{\Pr\left(Case\;2\right)}\left[\exp\left(-\lambda_S\pi 2A_{S,M}^{\frac{1}{\alpha_S}}x^{\frac{\alpha_M}{\alpha_S}}\right)-\right.\\&\left.\exp\left(-\lambda_S\pi 2B_{S,M}^{\frac{1}{\alpha_S}}x^{\frac{\alpha_M}{\alpha_S}}\right)\right],\end{aligned}\tag{22}$$

$$\begin{aligned}f_{X_S|Case\;2}=&\frac{f_{X_S}\left(x\right)}{\Pr\left(Case\;2\right)}\left[\exp\left(-\lambda_M\pi B_{M,S}^{\frac{2}{\alpha_M}}x^{\frac{\alpha_S}{\alpha_M}}\right)-\right.\\&\left.\exp\left(-\lambda_M\pi A_{M,S}^{\frac{2}{\alpha_M}}x^{\frac{\alpha_S}{\alpha_M}}\right)\right].\end{aligned}\tag{23}$$

3) The distance distribution of Case 4 is formulated as

$$f_{X_S|Case\,4}=\frac{\exp\left(-\lambda_M\pi A_{M,S}^{\frac{2}{\alpha_M}}x^{\frac{2\alpha_S}{\alpha_M}}\right)f_{X_S}\left(x\right)}{\Pr\left(Case\,4\right)}.\tag{24}$$

Proof: The detailed proofs of the distance distribution are similar to Lemma 4 in [10]. The proof is omitted due to space constraints. ■

C. Spectral Efficiency

Theorem 1: Based on the results of (9), (10) and (13) to (24), we take the SE of Case 2 UL as an example and the epression is given in equation (25).

$$\tau_2^U=\int_0^\infty f_{S|2}\int_0^\infty\Pr\left[H_{S,0}>\beta_{S,0}I_{U,2}x_S^{\alpha_S}\right]dtdx_S,\tag{25}$$

where $\beta_{S,0}=\left(e^t-1\right)/\left(P_V G_{S,0}\right)$, $I_{U,2}=I_{S,0}+I_{S,1}$. For the convenience of writing , we use $f_{S|2}\left(\cdot\right)$ to substitute $f_{X_S|Case\,2}\left(\cdot\right)$ and the following PDFs are simplified to the same form.

Proof: The SE of Case 2 UL is

$$\begin{aligned}\tau_2^U&=E\left[\ln\left(1+SINR_{U,S}\right)\right]\\&=\int_0^\infty f_{S|2}\int_0^\infty\Pr\left[\ln\left(1+\frac{P_V G_{V,0}H_{V,0}x_S^{-\alpha_S}}{I_{U,2}}\right)>t\right]dtdx_S\\&=\int_0^\infty f_{S|2}\int_0^\infty\Pr\left[H_{V,0}>\frac{\left(e^t-1\right)I_{U,2}}{P_V G_{V,0}}x_S^{\alpha_S}\right]dtdx_S\\&\overset{(a)}{=}\int_0^\infty f_{S|2}\int_0^\infty\Pr\left[H_{V,0}>\beta_{S,0}I_{U,2}x_S^{\alpha_S}\right]dtdx_S,\end{aligned}\tag{26}$$

where $\beta_{S,0}=\left(e^t-1\right)/\left(P_V G_{V,0}\right)$ in (a). The proof of $\Pr\left[H_{V,0}>\beta_{S,0}I_{U,2}x_S^{\alpha_S}\right]$ is

$$\begin{aligned}&\Pr\left[H_{V,0}>\beta_{S,0}I_{U,2}x_S^{\alpha_S}\right]\\&=E_{I_S}\left\{\Pr\left[H_{V,0}>\beta_{S,0}I_{U,2}x_S^{\alpha_S}\right]\right\}\\&\overset{(a)}{=}E_{I_S}\left[\frac{\Gamma\left(m_S,m_S\beta_{S,0}I_{U,2}x_S^{\alpha_S}\right)}{\Gamma\left(m_S\right)}\right]\\&\overset{(b)}{=}E_{I_S}\left[\sum_{k=0}^{m_S-1}\frac{\left(m_S\beta_{S,0}I_{U,2}x_S^{\alpha_S}\right)^k}{k!}e^{-m_S\beta_{S,0}I_S x_S^{\alpha_S}}\right]\\&=\sum_{k=0}^{m_S-1}\frac{\left(-m_S\beta_{S,0}x_S^{\alpha_S}\right)^k}{k!}\left[\frac{\delta^k}{\delta j^k}\zeta_{I_{U,2}}\left(j\right)\right]_{j=m_S\beta_{S,0}x_S^{\alpha_S}},\end{aligned}\tag{27}$$

where (a) follows from the CCDF of gamma random variable $H_{V,0}$, and (b) follows from the definition of incomplete gamma function for integer values of m_S. The aggregate interference can be devided into two independent components $I_{V,0},I_{V,1}$, the Laplace transform of interference can be computed as product of the Laplace transforms of the two components, thus, $\zeta_{I_{U,2}}\left(j\right)=\zeta_{I_{V,0}}\left(j\right)\zeta_{I_{V,1}}\left(j\right)$. Similar to the proof of Lemma 5 in [14], the Laplae transfroms of $I_{V,0}$ and $I_{V,1}$ are

$$\begin{aligned}&\zeta_{I_{V,0}}\left(j\right)\\&=E_{I_{V,0}}\left[\exp\left(-jI_{V,0}\right)\right]\\&=E_{I_{V,0}}\left[\exp\left(-j\sum_{x_S\in\Xi_{l_0}^V\setminus[-x_S,x_S]}P_V G_{V,0}H_{V,0}x^{-\alpha_S}\right)\right]\\&\overset{(a)}{=}E_{\Xi_{l_0}^V\setminus X^*}E_{H_{V,0}}\left[\prod_{x_S\in\Xi_{l_0}^V\setminus[-x_S,x_S]}e^{-jP_V G_{V,0}H_{V,0}x^{-\alpha_S}}\right]\\&\overset{(b)}{=}\exp\left[-2\lambda_V\int_{x_S}^\infty\left(1-\left(1+\frac{jP_V G_{V,0}x^{-\alpha_S}}{m_S}\right)^{-m_S}\right)dx\right],\end{aligned}\tag{28}$$

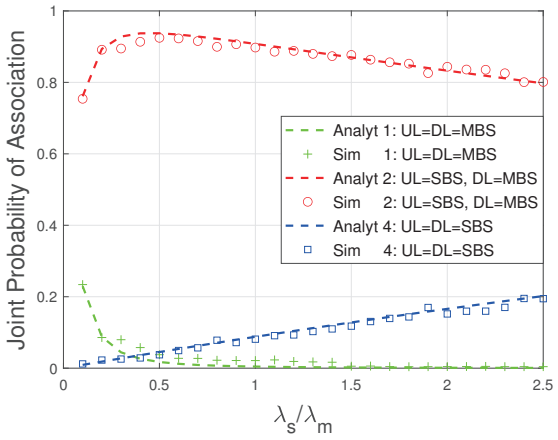

(a) LOS

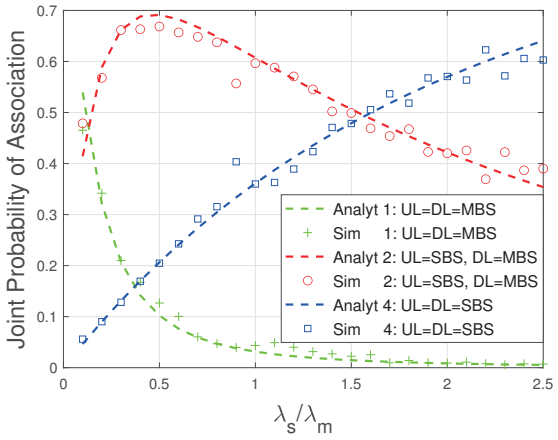

(b) NLOS

Fig. 2. Joint association probability for Cases $1-4$ ($P_M = 46\ dBm; P_S = 20\ dBm; P_V = 20\ dBm$).

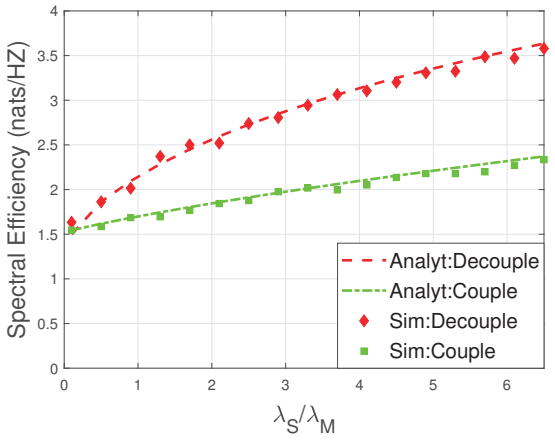

(a) LOS

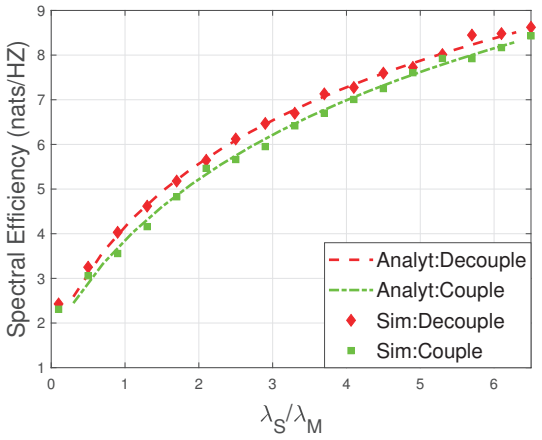

(b) NLOS

Fig. 3. System average SE for decoupled and coupled cases in LOS and NLOS scenarios.

where (a) follows from the independence of $\Xi_{l_0}^V$, we convert the accumulative form into accumulative multiplication. (b) follows from the Nakagami-m fading assumption and the PGFL of a 1D PPP. Similarly, the proof of $\zeta_{I_{S,1}}$ can be derived by following the same steps. ■

Based on the results of (13) to (25), the other links' expressions of SE can be derived by following the similar steps of Theorem 1 in UL/DL decoupled C-V2X.

The average system SE of UL/DL decoupled C-V2X is

$$SE = \sum_{i=1}^{4} \sum_{n}^{\{U,D\}} \tau_{Case\,i}^{n} Pr\left(Case\ i\right), \tag{29}$$

where $\tau_{Case\,i}$ is the SE of Case i's n-link, here $i \in \{1,2,4\}$, $n \in \{U,D\}$.

The SE of coupled access could be derived as Corollary 2 in [10].

IV. NUMERICAL RESULTS

In this section, more than 100000 Mento Carol simulations are executed in a UL/DL decoupled access C-V2X scenario that the simulation observation area is a circular area with a radius of 5 km for line of sight (LOS) and non line of sight (NLOS). A comprehensive SE comparison between coupled and decoupled access modes is presented. Table I shows the default system parameters and the values of the simulation follow [10]. Compared with the empirical results from Monte-Carlo simulations, the accuracy of the theoretical results is verified in Fig. 2 and Fig. 3.

TABLE I
SYSTEM PARAMETERS

Parameters	Value
Macro BS transmit power P_M (dBm)	46
Small BS transmit power P_S (dBm)	20
Vehicle transmit power P_V (dBm)	20
Pathloss exponent for MBS α_M	4
Pathloss exponent for SBS α_S(NLOS)	4
Pathloss exponent for SBS α_S(LOS)	2
Antenna Gain for MBS G_M(dBi)	0
Antenna Gain for vehicle in typical line G_{S0} (dBi)	0
Antenna Gain for vehicle in other line G_{S1} (dBi)	-20
Line density λ_l (1/km)	10

We first analyze the joint association probabilities of three cases as shown in Fig. 2(a) and Fig. 2(b). The joint association probability is equal to the percentage of vehicles that choose the particular case. According to Fig. 2(a) and Fig. 2(b), we observe that in UL/DL decoupled C-V2X networks, the probability of vehicles choosing Case 2 to communicate increases rapidly at the beginning, then decreases slowly at the cost of the increase in association Case 4 i.e., when vehicles choose to connect with SBSs in both UL and DL, as the ratio of the density of SBS and MBS increases in both LOS and NLOS. The probability of Case 4 is increasing all the time in both LOS and NLOS. The reason behind this phenomenon is obvious, with the increasing density of SBS, the SBSs are getting closer to the vehicles and the closer distance makes up for the disadvantage of lower power compared with MBS.

Fig. 3 shows the main result i.e., the comparison of the decoupled and coupled average system SE in LOS and NLOS. It shows that the SE is improved both in LOS and NLOS after being decoupled. Specifically, we can see that the improvement is increasing as the ratio of the density of SBS and MBS increases in LOS and the performance is nearly increased by 50% in LOS. While in NLOS, the improvement is very small. UL/DL decoupled access separates UL from DL, UL could be connected to the BS with the largest signal power, but not the DL'BS that may not have the largest signal power in UL. Therefore, the improvement of SE mainly comes from UL. In NLOS, according to Fig. 2(a), most vehicles choose Case 2 i.e., when vehicles choose to connect with MBS in DL and SBS in UL, thus the SE improvement comes from UL'SBS and most vehicles connect to MBS in coupled mode, thus SE has a higher improvement as the ratio of SBS and MBS increase. While in NLOS, most vehicles choose Case 4 as the SBS increases, therefore, the improvement which comes from Case 2's UL is very small, thus the system average SE's improvement is not obvious. This phenomenon suggests that UL/DL decoupled access could bring gains compared to traditional coupled access and this technology can be used as a tool for achieving higher SE, especially in the LOS scenario in C-V2X.

V. Conclusion

In this paper, we have proposed a UL/DL decoupled C-V2X networks analytical framework and modeled it as a Cox process for analyzing the SE of the UL/DL between vehicles and MBSs/SBSs. Specifically, we have analyzed the joint association probability, distance distributions to its serving BSs and the SE of all links in UL/DL decoupled C-V2X networks. Theoretical analysis and empirical results have verified the effectiveness of the proposed analytical framework and demonstrated that with UL/DL decoupled access in C-V2X, better system average SE can be achieved than coupled access both in LOS and NLOS. For the future work, we will focus on the mobility management and joint access optimization in UL/DL decoupled C-V2X.

Acknowledgment

This work is supported in part by the National Natural Science Foundation of China (No. 61871211), in part by the Summit of the Six Top Talents Program of Jiangsu Province and in part by the Innovation and Entrepreneurship of jiangsu Province High-level Talent Program.

References

[1] Y. Gu, L. X. Cai, M. Pan, L. Song, and Z. Han, "Exploiting the Stable Fixture Matching Game for content sharing in D2D-Based LTE-V2X Communications," in *2016 IEEE Global Communications Conference (GLOBECOM)*, 2016, pp. 1–6.

[2] K. Abboud, H. A. Omar, and W. Zhuang, "Interworking of DSRC and cellular network technologies for V2X communications: A survey," *IEEE transactions on vehicular technology*, vol. 65, no. 12, pp. 9457–9470, 2016.

[3] F. Boccardi, J. Andrews, H. Elshaer, M. Dohler, S. Parkvall, P. Popovski, and S. Singh, "Why to decouple the uplink and downlink in cellular networks and how to do it," *IEEE Communications Magazine*, vol. 54, no. 3, pp. 110–117, 2016.

[4] H. Zhou, W. Xu, J. Chen, and W. Wang, "Evolutionary V2X technologies toward the internet of vehicles: challenges and opportunities," *Proceedings of the IEEE*, vol. 108, no. 2, pp. 308–323, 2020.

[5] R. Li, K. Luo, T. Jiang, and S. Jin, "Uplink spectral efficiency analysis of decoupled access in multiuser MIMO HetNets," *IEEE Transactions on Vehicular Technology*, vol. 67, no. 5, pp. 4289–4302, 2018.

[6] J. G. Andrews, A. K. Gupta, and H. S. Dhillon, "A primer on cellular network analysis using stochastic geometry," 2016.

[7] K. Yu, H. Zhou, B. Qian, Z. Tang, and X. Shen, "A reinforcement learning aided decoupled RAN slicing framework for cellular V2X," in *GLOBECOM 2020-2020 IEEE Global Communications Conference*. IEEE, 2020, pp. 1–6.

[8] K. Rabieh, M. Pan, Z. Han, and V. Ford, "SRPV: A Scalable Revocation Scheme for Pseudonyms-Based Vehicular Ad Hoc Networks," in *2018 IEEE International Conference on Communications (ICC)*, 2018, pp. 1–6.

[9] Y. Yao, X. Chang, J. Mišić, V. B. Mišić, and L. Li, "Bla: Blockchain-assisted lightweight anonymous authentication for distributed vehicular fog services," *IEEE Internet of Things Journal*, vol. 6, no. 2, pp. 3775–3784, 2019.

[10] Z. Sattar, J. V. Evangelista, G. Kaddoum, and N. Batani, "Spectral efficiency analysis of the decoupled access for downlink and uplink in two-tier network," *IEEE Transactions on Vehicular Technology*, vol. 68, no. 5, pp. 4871–4883, 2019.

[11] L. Zhang, W. Nie, G. Feng, F.-C. Zheng, and S. Qin, "Uplink performance improvement by decoupling uplink/downlink access in HetNets," *IEEE Transactions on Vehicular Technology*, vol. 66, no. 8, pp. 6862–6876, 2017.

[12] K. Smiljkovikj, P. Popovski, and L. Gavrilovska, "Analysis of the decoupled access for downlink and uplink in wireless heterogeneous networks," *IEEE Wireless Communications Letters*, vol. 4, no. 2, pp. 173–176, 2015.

[13] V. V. Chetlur and H. S. Dhillon, "Coverage analysis of a vehicular network modeled as Cox process driven by poisson line process," *IEEE Transactions on Wireless Communications*, vol. 17, no. 7, pp. 4401–4416, 2018.

[14] Chetlur, Vishnu Vardhan and Dhillon, Harpreet S, "Coverage and rate analysis of downlink cellular vehicle-to-everything (C-V2X) communication," *IEEE Transactions on Wireless Communications*, vol. 19, no. 3, pp. 1738–1753, 2019.

[15] B. Qian, H. Zhou, T. Ma, Y. Xu, K. Yu, X. Shen, and F. Hou, "Leveraging dynamic stackelberg pricing game for multi-mode spectrum sharing in 5G-VANET," *IEEE Transactions on Vehicular Technology*, vol. 69, no. 6, pp. 6374–6387, 2020.

[16] M. N. Sial, Y. Deng, J. Ahmed, A. Nallanathan, and M. Dohler, "Stochastic geometry modeling of cellular V2X communication over shared channels," *IEEE Transactions on Vehicular Technology*, vol. 68, no. 12, pp. 11 873–11 887, 2019.